Electrospun Nanocomposites from Polystyrene Loaded with Cellulose Nanowhiskers

Orlando J. Rojas, Gerardo A. Montero, Youssef Habibi

Forest Biomaterials Laboratory, North Carolina State University, Raleigh, North Carolina

Received 2 October 2008; accepted 11 January 2009
DOI 10.1002/app.30011
Published online 30 March 2009 in Wiley InterScience (www.interscience.wiley.com).

ABSTRACT: Composite microfibers from polystyrene and cellulose nanowhiskers were produced by electrospinning. The morphology of the microfibers was examined by using scanning and transmission electron microscopies. Surface porosity, unique ribbon-shapes, and the presence of twists along the fiber axis were observed in the composite microfibers. Thermomechanical properties of processed nanocomposites were studied by differential scanning calorimetry and dynamical mechanical analyses. The reinforcing effect of cellulose nanowhiskers was confirmed as the glassy modulus of electrospun microfibers increased with nanowhisker load. This effect is explained to be the result of mechanical percolation of cellulose nanowhiskers forming a stiff and continuous network held by hydrogen bonding. It is demonstrated that cellulose nanoparticles can be used effectively to reinforce hydrophobic matrices and to produce unique structural properties, enabling new functionalities and properties. © 2009 Wiley Periodicals, Inc. J Appl Polym Sci 113: 927–935, 2009

Key words: cellulose; electrospinning; mechanical properties; microfibers; nanocomposites; nanoparticles

INTRODUCTION

Electrostatic fiber spinning or "electrospinning" is a versatile method to manufacture fibers with diameters ranging from several microns down to 100 nm or less through the action of electrostatic forces. During the electrospinning process, a charged fluid jet from a polymer solution is extruded under an applied electric field between two electrodes. Fluid extension occurs first in uniform, straight flow lines to then undergo vigorous whipping motion caused by electrohydrodynamic instabilities. As solvent in the jet solution evaporates, the polymer is collected onto a grounded substrate to form a nonwoven mat or network with significant large surface-to-volume ratios. Electrospinning has recently received great attention in the fabrication of polymer nanofibers in a wide range of applications that demand high-performance fibers in clothing, filtration, and biomedical materials. Other opportunities for electrospun fibers and ensuing structures include the fabrication of scaffolds for tissue engineering, in drug delivery, biosensors, and electronic and semi-conductive materials. Several excellent reviews of the state-of-the-art in the field of electrospinning, electrospun fibers, properties, and applications have been published.[1–5] High-throughput electrospinning units are expected to open further the opportunities for electrospun nonwovens.[6–9]

Electrospinning is a simple and easy to control technique. However, the various concurrent phenomena taking place during whipping make difficult to draw a clear cut correlation between instrument design and operational conditions and the characteristics of the produced micro or nanofibers. Processing parameters such as the voltage and distance between the spinning tip and the collector, the properties (conductivity, viscosity, density, surface tension, etc.) of the spinning solution, and its flow rate can drastically affect the outcome of the spinning process.

Electrospinning has been used in the manufacture of ultrafine fibers from such polymers as polyolefins, polyamides, polyesters, polyurethanes, polypeptides, and DNA as well as polymers with special properties, such as conductive macromolecules. Because of its wide-spread applications polystyrene (PS) has largely been used to fabricate nanofibers. Studies on the relation among electrospinning parameters, solvent type, and the presence of additives and the processability of polystyrene during electrospinning have been reported.[10–16] Composite eletrospun micro and nanofibers of polystyrene incorporating nanosized fillers have also attracted great interest. For example, gold nanoparticles[17] and multiwalled carbon nanotubes[18,19] were used in electrospun PS

Correspondence to: Y. Habibi (yhabibi@ncsu.edu).
Contract grant sponsor: National Research Initiative of the USDA Cooperative State Research, Education and Extension Service; contract grant number: 2007-35504-18290.

fibers. Such nanofibers are found to be valuable in high-performance applications that require ultra high surface areas and special material properties.

Recently, the use of reinforcing nanosized cellulose nanowhiskers has been at the central stage of efforts by several groups working on the development of nanocomposites. Such cellulose nanoparticles offer a number of advantages including their high aspect ratio and surface area, unique morphology as well as excellent mechanical and thermal properties.[20] In addition to their unique chemical and surface characteristics as well as their biodegradability, cellulose nanowhiskers offer the advantage of being derived from renewable resources.

In this study, we demonstrate the incorporation of cellulose nanowhiskers in electrospun polystyrene-based microfibers. To fine-tune the compatibility between the cellulose nanoparticles and the polymeric matrix, a nonionic surfactant was used. This approach ensured the stabilization of the hydrophilic cellulose whisker dispersion in the precursor hydrophobic matrix. The morphology of the resulting microfiber webs were characterized by using scanning and transmission electron microscopy, whereas the thermal and mechanical properties were accessed via differential scanning calorimetry and dynamic mechanical analysis, respectively. Overall, this effort is anticipated to inspire new opportunities for cellulose nanocrystals in composite electrospun fibers and to enable special functionalities and properties of the resulting materials.

EXPERIMENTAL

Materials and methods

Polystyrene (Mw = 230,000), Whatman® No.1 cellulose filter paper, hydrochloric acid, and nonionic surfactant sorbitan monostearate were purchased from Sigma-Aldrich (St. Louis, MO). Tetrahydrofuran (THF) was obtained from B&J Brand™ (Muskegon, MI). All chemicals were of analytical grade and used as received.

Preparation of cellulose nanowhiskers

Cellulose nanowhiskers (CNW) were prepared by HCl-assisted hydrolysis of Whatman® cellulose filter paper. Typically, 20 g of filter paper were dispersed using Osterizer® blender in 700 mL aqueous 1.5*M* HCl solution after which cellulose hydrolysis was allowed during 4 h at 100°C. After the hydrolysis, the suspension was diluted using deionized water and centrifuged several times at 2800 rpm until ensuring neutral pH of the cellulose dispersion. Following, the CNWs were resuspended in water and subjected to centrifugation at higher spinning rates. Centrifugation at 8000 rpm for 30 min followed by centrifugation at 14,000 rpm for additional 30 min (using an Automatic Servall® Superspeed Centrifuge) was performed to minimize the span in the particle size distribution of the collected CNW. The pelleted CNWs obtained after the last centrifugation step were dried using a freeze dry/shell freeze system (Labconco, Kansas City, MU). The average length and width of the obtained CNWs were 200 nm and 10–20 nm, as determined by AFM (Q-Scope 350 AFM, Quesant Instruments, Santa Cruz, CA). We note the uncertainly in these determinations due to AFM tip-broadening artifacts that usually lead to an overestimation of the dimensions.

Polymer dispersion

The cellulose nanowhiskers (CNW) obtained after hydrolysis and the separation procedures described before were dispersed in THF under sonication. Equal amounts of nonionic sorbitan monostreate surfactant (S) were also added. The respective volume of polystyrene (PS) dissolved in THF were mixed with the CNW dispersion and the resulting suspensions were agitated overnight before electrospinning. The final concentration of PS used to electrospin microfibers was varied from 10 to 30% and CNW was added at two weight ratios relative to PS and S (PS : CNW of 94 : 6 and 91 : 9). We note that the composition used in our systems was optimized in terms of the colloidal stability of the dispersion and also from the ensuing mechanical properties of composites obtained by film casting.[21]

The viscositiy, conductivity, and surface tension of the final solutions were determined at 25°C by a programmable rheometer (Brookfield, DV-III Ultra), conductivity meter (Corning Inc., model 441), and the du Noüy ring method (Fisher tensiomat, model 21), respectively. The properties of different materials are summarized in Table I.

Electrospinning

Electrospinning of the dispersions was carried out using a custom made electrospinning device with a vertical, uniform electric field generated between two (top and bottom) parallel circular electrodes. The electrospinning setup included a high-voltage power supply unit (Series EL, Glassman High Voltage) with power range from 0 to 50 DC kV, a syringe pump (Aldrich) controlled by a Pump-term computer code. In a typical electrospinning experiment, high voltage was applied to the polymer dispersion by connecting the tip of a metal syringe needle (gauge 22) directly to the power supply. Collectors consisting of a circular aluminum plate (16 cm diameter) or a rotating mandril (12 and 8.5 cm

TABLE I
Properties of THF Solvent and Respective Dispersions (20% (w/v) Ps Base solutions)

Properties	Solvent (THF)	PS	PS : CNW : S (94 : 6 : 6)	PS : CNW : S (91 : 9 : 9)
Viscosity (mPa s)[a]	0.5	264	329	398
Conductivity (μS/cm)[a]	0	0	10	10
Surface Tension (mN/m)[a]	23.5	31.3	31.7	32.3

[a] Measured at 25°C.

length and outer diameter, respectively) covered by aluminum foils were used to collect nonwovens of the electrospun microfibers. The collectors were placed at a given distance away from the tip of the needle. Electrospinning was conducted under ambient temperature and flow rate, spinning voltage, and working distance were varied depending on the composition of the precursor dispersion and the observed whipping motion of the fluid jet.

Scanning electron microscopy (SEM)

A Hitachi S-3200N variable pressure SEM was used to obtain microphotographs of the composite nanofibers formed after electrospinning. The nanofibers, which were collected on the aluminum foils, were shadowed with a layer (~ 150 Å thick) of gold-palladium (Au/Pd) and observed with a working distance between 3 and 60 mm using an accelerating voltage from 0.3 to 30 kV.

Transmission electron microscopy (TEM)

A Hitachi HF-2000 Transmission Electron Microscopy (TEM) was used to analyze some of the nanofibers produced. The TEM used a cold field emission electron source at an accelerating voltage of 200 kV. This electron source delivered an electron beam with a small energy spread and excellent coherency that helped to improve image resolution. The nanofibers were sprayed or deposited onto 3-mm mesh copper TEM grids that were placed on the bottom collector plate while whipping oscillations during the electrospinning process occurred.

Differential scanning calorimetry (DSC)

Around 10 mg of electrospun fiber samples were placed in a DSC cell (DSC Q200 from TA Instruments, New Castle, DE). Each sample was heated from 25 to 250°C at a heating rate of 10°C min^{-1}. The glass transition temperature T_g was taken as the inflection point of the specific heat increment at the glass-rubber transition.

Dynamic mechanical analysis (DMA)

A Dynamic Mechanical Analyzer (DMA 2980 from TA Instruments) was used to measure the mechanical properties of the composite nanofibers under tension as a function of temperature. The samples were prepared by cutting 5-mm width strips from the nanofibers films collected on the rotating mandril. All the measurements were carried out at a constant frequency of 1 Hz with strain amplitude of 0.07% using a sample gap distance of 10 mm. The temperature range was −100 to 200°C with a heating rate of 3°C/min. DMA tests were carried out by duplicate with an observed experimental error of about ± 3%.

RESULTS AND DISCUSSION

Morphology of electrospun composite microfibers

Polymer (PS) solutions in THF containing 0, 6, and 9 wt % of CNWs were used for electrospinning. Sorbitan monostearate was added to improve the dispersion and compatibility of the hydrophilic cellulose nanowhiskers with the hydrophobic polystyrene matrix. From our previous work with nanocomposite films prepared by the casting-evaporation technique, it was observed that CNW with surfactant added at equal weight ratios gave the best dispersion and compatibility results.[21] Therefore the same conditions were used in this work. However, the concentration of PS was varied from 10 to 30 wt % of the total composite blend which was the range we found suitable for electrospinning. The morphology of the electrospun microfiber webs were characterized by scanning electron microscopy and transmission electron microscopy.

The 10 and 20% solutions of PS dissolved in THF were easily electrospun, whereas the 30% solution was difficult to process because of the high viscosity of the solution, which caused material clogging at the spinneret's tip. This effect was due to the rapid evaporation of the high vapor pressure THF (boiling point of 66°C) at the hanging droplets that generated the spinning jet.

Beading was observed in microfibers produced from PS solution concentration of 10% (at all applied voltages) and 20% (voltage strength below 20 kV) [see Fig. 1(A)]. The presence of similar bead

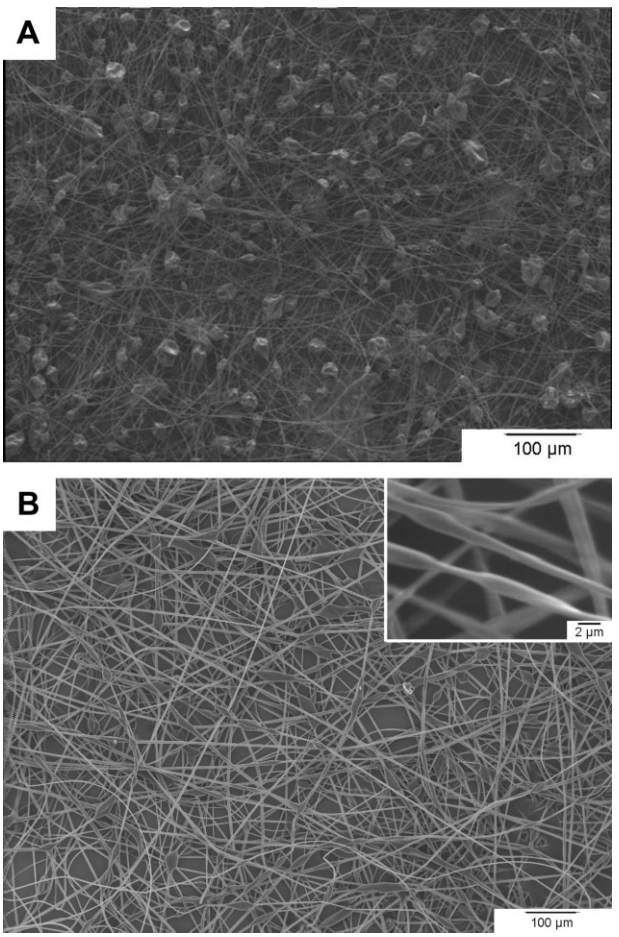

Figure 1 SEM micrographs of PS electrospun microfibers obtained at 20 kV (A) and 40 kV (B) by using 20% PS concentration in THF and a flow rate (Q) of 0.2 mL/min (distance between electrodes was 16 cm). Inset in 1B: A magnified image of ribbon-shape structures in the formed nonwoven.

morphologies has been reported for electrospun polystyrene microfibers.[10] However, the 20 wt % PS solutions formed electrospun microfibers at relatively high voltage (40 kV) at flow rate of 0.2 mL/min. Under this condition, the fibers were bead-free and exhibited ribbon-like morphologies [see Fig. 1(B)]. The diameter of the resulting PS microfibers ranged from 1 to 8 μm.

When cellulose nanowhiskers (CNWs) were added to the PS matrix in the absence of any surfactant [but the under conditions used for bead-free PS microfibers, as shown in Fig. 1(B)], the produced webs contained a large density of beads. These results along with those for other loadings are reported in Table II and are also illustrated in the respective SEM micrographs [see Fig. 2(A)]. We note that efforts to minimize the formation of beads (by adjusting the operating conditions and polymer concentrations) were unsuccessful. This was probably the result of poor dispersion or compatibility of the CNWs in the precursor PS solution. Significantly, the addition of nonionic surfactant to the PS-CNW dispersions improved their stability and minimized (or prevented) the presence of beads in the resulting web, depending on the electrospinning conditions [Fig. 2(B)].

Lin et al.[11] reported that the formation of beaded fibers from PS polymer was attributed to an insufficient stretch of the filaments during the whipping of the jet, because of a low electrical charge density. They observed that the addition of small amounts of a cationic surfactant prevented the formation of beaded fibers during electrospinning.[11] Such effects have been also reported in the case of systems with nonionic surfactants; for example, it has been reported that the addition of nonionic Triton X-405 reduced the bead number density and also changed the morphology of PS fibers.[11]

After optimizing the electrospinning conditions to generate bead-free fiber webs (40 kV, collector-to-tip distance of 16 cm and flow rate of 0.2 mL/min), we found that the diameter of the resulting electrospun PS microfibers depended on the CNW load. The range of diameters of the composite (PS-CNW) fibers were measured to be 1.6 to 5.4 μm and 0.5 to 2 μm for CNW loads of 6% and 9%, respectively, (with surfactant added at loads equal to CNW concentrations) (see Table I). The reduction in the microfiber diameter is explained by the improved interaction

TABLE II
Electrospinning Conditions and Fiber Morphologies of CNW-Loaded Ps Composites With and Without Nonionic Surfactant (S)

Composite PS : CNW : S	PS Concentration (wt %)	Voltage (kV)	Distance (cm)	Flow rate (mL/min)	Fiber diameter (μm)	Observations
94 : 6 : 0	20	30	16	0.15	~ 0.86–2.8	Beading
94 : 6 : 0	20	35	16	0.15	~ 0.90–2.9	Beading
94 : 6 : 0	20	40	16	0.15	~ 1.0–2.8	Beading
94 : 6 : 6	20	35	16	0.15	~ 0.75–2.5	Beading
94 : 6 : 6	20	40	16	0.15	~ 1.2–3.7	Less beading
94 : 6 : 6	20	40	16	0.20	~ 1.6–5.4	No beads
94 : 6 : 6	20	45	16	0.20	~ 1.9–4.3	No beads + surface pores
91 : 9 : 9	20	40	16	0.20	~ 0.6–2.0	No beads

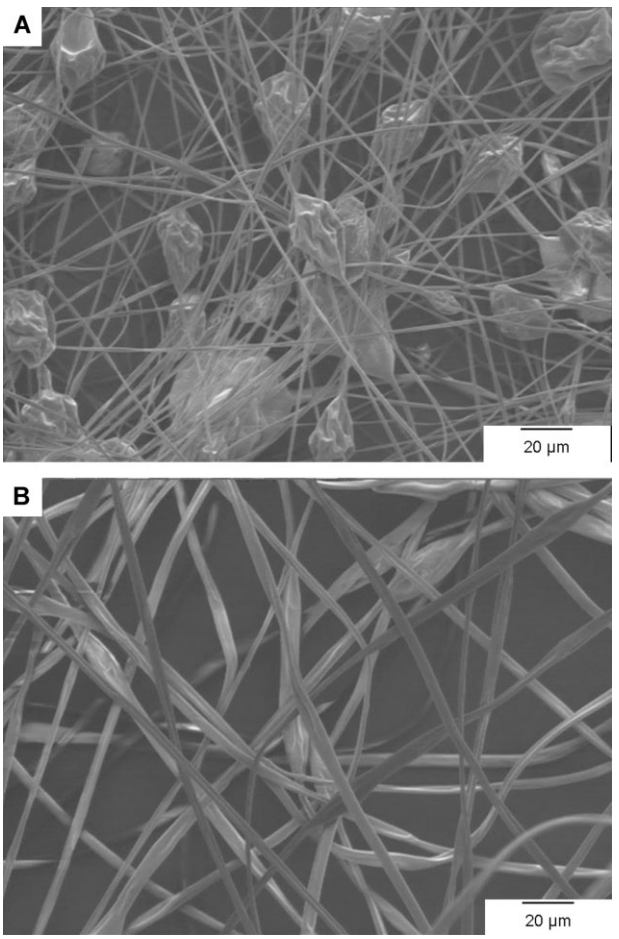

Figure 2 SEM micrographs of PS/CNW electrospun microfiber composites loaded with 6% CNW in the absence of surfactant (A) and with surfactant added (6% of total) (B). The operating conditions were 20% PS in THF, $Q = 0.2$ mL/min, 40 kV, distance = 16 cm.

between PS-chains and the CNWs in the presence of surfactant and also by the reduction in surface tension. In the absence of CNWs, the nonionic surfactant induced a reduction in the diameter of the electrospun PS microfibers.

We observed that neat PS microfibers were flat or ribbon-like as has been reported in experiments with PS and others polymers.[22–32] Koombhongse et al.[22] described ribbon-shaped electrospun fibers from 30 wt % PS in dimethylformamide, 10 wt % poly(ether imide) in hexafluoro-2-propanol, and 20 wt % poly(2-hydroxyethyl methacrylate) in ethanol. Furthermore, ribbon-like nanofibers of barium titanate[33] were observed after electrospinning a solution containing barium-titanium alkoxide precursor and poly(vinyl pyrrolidone) after calcination in air. This morphological feature has been rationalized in terms of specific conditions such as electrospinning voltage and solution properties.

A unique attribute in the present system of PS microfibers filled with CNW was the presence of

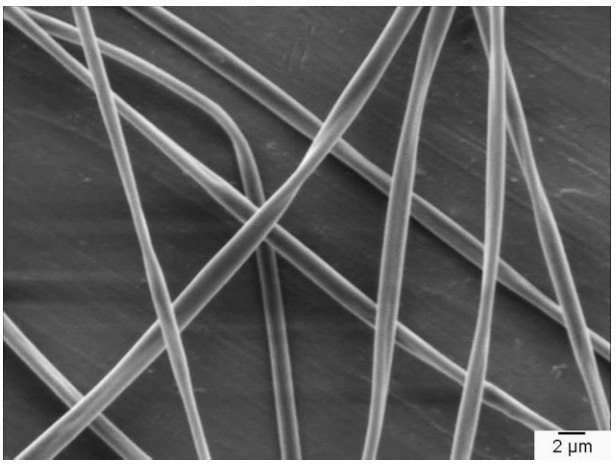

Figure 3 SEM of electrospun PS microfibers filled with 6% CNWs in the presence of nonionic surfactant (PS : CNW : S of 94 : 6 : 6) showing ribbon-shape structures. The operating conditions were 20% PS in THF, $Q = 0.2$ mL/min, 40 kV, distance = 16 cm.

twists along the fiber axis, as shown in Figure 3. Distinctive twist nodes can be seen regularly in each electrospun fiber. Furthermore, SEM observation indicated that the CNW load did not affect the periodicity or distance between twist nodes in the microfibers.

The physical properties of the spinning solvent and the evaporation rate during the electrospinning process (which is influenced by the applied voltage) are mainly responsible for the production of ribbon-shaped fibers. However, the mechanism of formation of ribbon-shaped fibers and the conditions triggering fiber twisting is not understood. We hypothesize that the low boiling point of THF and the relatively

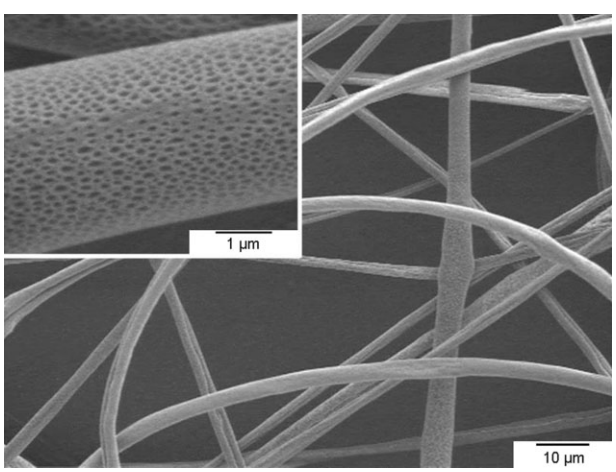

Figure 4 SEM of electrospun PS microfibers filled with 6% CNWs in the presence of nonionic surfactant (PS : CNW : S of 94 : 6 : 6) showing ribbon-shape structures and the formation of surface pores of 20–60 nm (short axis) to 120–300 nm (long axis) obtained after electrospinning at high voltages. The operating conditions were 20% PS in THF, $Q = 0.2$ mL/min, 45 kV, distance = 16 cm.

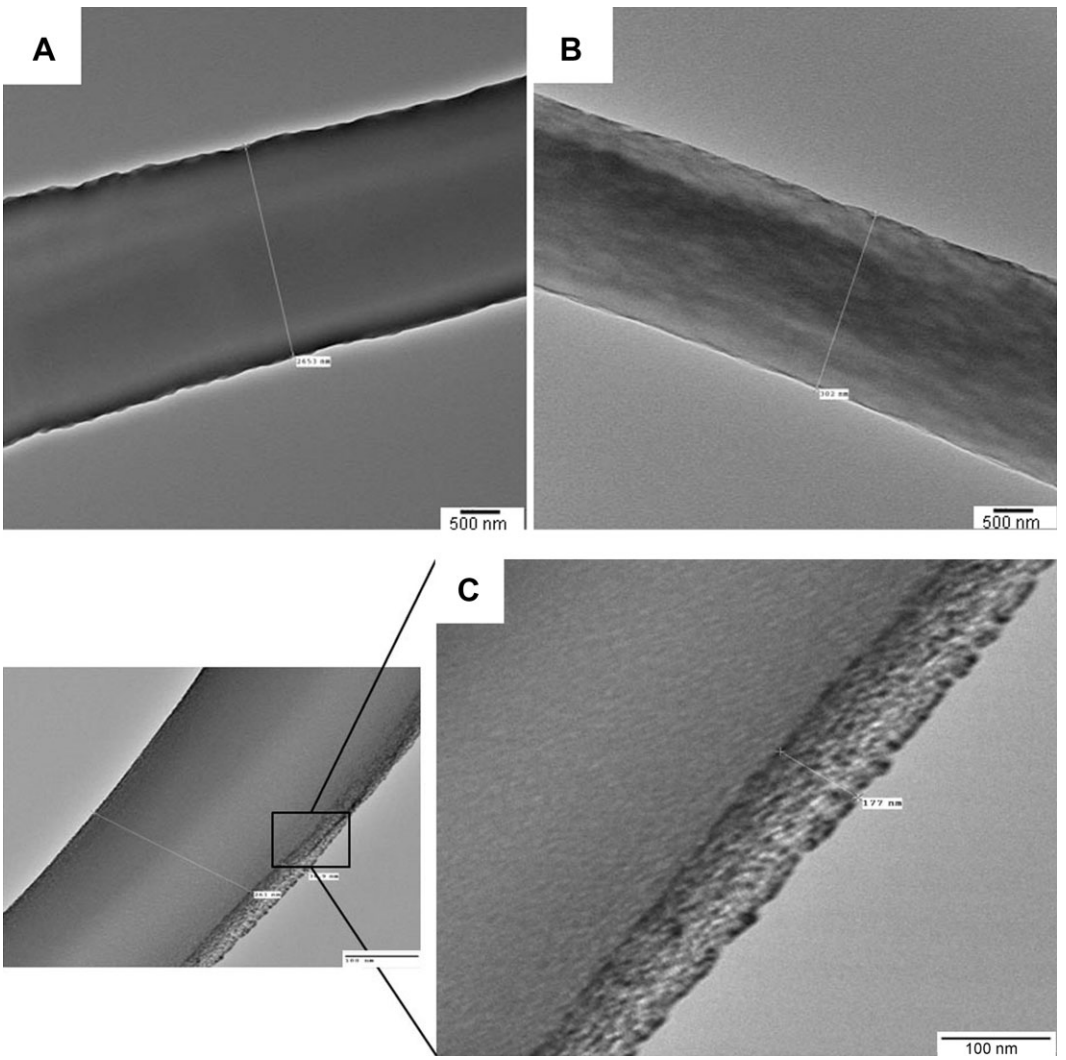

Figure 5 TEM of electrospun microfibers from neat PS (A) and from PS filled with 9% CNWs in the presence of equivalent amount of nonionic surfactant (B, C). Operating conditions: 20% PS in THF, $Q = 0.2$ mL/min, 40 kV, distance = 16 cm. Scale bars correspond to 500 nm (A) and 100 nm (B&C).

high voltage used in our experiments with electrospinning favored the formation of ribbon structures.

An additional issue that became evident was fiber surface roughening when the electrospinning voltage exceeded 40 kV, as illustrated in Figure 4. Specifically, the formation of surface (oval) pores on the fibers appeared to be related to the fast evaporation rate of the solvent under high voltages. For the processing conditions used in Figure 4, it was found that the dimensions of the surface oval pores ranged 20–60 (short axis) to 120–300 nm (long axis). Similar features were obtained when electrospinning was run under slightly negative ambient pressures (which increased the rate of solvent evaporation). We note that Megelski et al.[34] reported on the production of 5–15 μm diameter microfibers from electrospinning PS (18 to 35 wt %) in THF solvent and also described the formation of surface pores of 50 to 150 nm size. Likewise, Liu[35] observed the formation of porous fibers when electrospinning isotactic poly(methyl methacrylate) and polystyrene dissolved in a relatively volatile solvents (such as methylene chloride and THF, respectively). Dalay et al.[36] reported an experimental and theoretical study involving the formation of porous structures in electrospun fibers made from the same polymers and they concluded that formation of porous fibers were favored if the solvent utilized was volatile and sensitive to moisture absorption.

FTIR and surface analyses carried out with the X-ray electron spectroscopy confirmed the presence of CNW in the composite microfibers. Transmission electron microscopy was also used to analyze the microfibers in terms of the presence and distribution of CNWs in the PS fiber matrix. Figure 5 shows high magnification TEM micrographs of neat PS microfibers [Fig. 5(A)] and PS microfibers loaded with 9% of CNW [Fig. 5(B)]. Under same observation

conditions, the PS microfibers exhibited a smooth surface and were relatively clear, whereas the PS microfibers containing CNW were rougher and darker. This observation may be related to the presence of CNW; however, identification of CNWs inside the fibers was not possible because of the low contrast, even at very high magnification. We note further that the addition of uranyl acetate staining agent to the dispersion before electrospinning did not improve this contrast. Because of the nature of the specimens collected (nonwoven structures) and also because their small thicknesses, the alternative of using ultrafine cross sections to identify internal features is extremely challenging and was not attempted in this study.

An outer layer of $\sim$ 100–200 nm thickness was observed on the surface of the microfibers loaded with CNW, which was not present in the case of microfibers obtained from neat PS [Fig. 5(C)]. It is hypothesized that this outer layer contains CNW that accumulated in the periphery under the electrospinning conditions. The density of CNW is slightly higher than that of PS. Therefore, one could expect partitioning of the two phases under high centrifugal fields. Additionally, differences in surface energies are also anticipated to contribute to this effect. However, we are not certain as to the dominant mechanism. Because of the low contrast between PS and CNW we cannot conclusively describe the surface and internal morphology of the microfibers. However, the presence of CNW inside the fibers cannot be ruled out. In fact, the improved mechanical properties of the fibers reinforced with cellulose nanoparticles provide indirect indication of their effect (see next section).

Thermomechanical properties of electrospun composite microfibers

DSC and DMA measurements were carried out to study the thermomechanical properties for the composite electrospun microfibers. Figure 6 shows the DSC thermograms obtained for microfibers from neat PS and PS loaded with CNW in the presence of nonionic surfactant. The thermogram profiles are all similar to those obtained for the PS-CNW-S composites obtained by film casting, as we reported elsewhere.[21] However, a distinctive feature was observed in the glass transition temperature T_g obtained for electrospun PS microfibers (ca. 78°C): The T_g was lower than that obtained for casted PS films (93°C). This phenomenon is probably related to the structural modifications that resulted from the high voltage used during electrospinning. Similar trends have been shown in other electrospun polymers.[37] We also note that the T_g of PS fiber with added CNW (and surfactant) tended to decrease

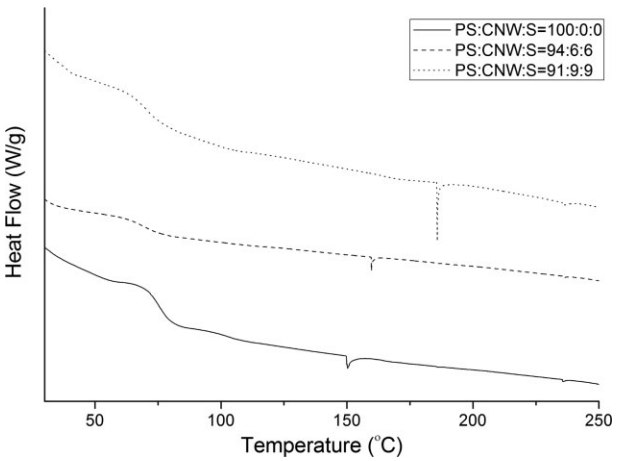

Figure 6 DSC thermograms for electrospun microfibers collected as a nonwoven on a rotating mandril collector of neat PS (100 : 0 : 0) and PS loaded with 6 and 9% cellulose whiksers (CNW) in the presence of equivalent amount of nonionic surfactant (S). The electrospinning operating conditions were 20% PS in THF, $Q = 0.2$ mL/min, 40 kV, distance = 16 cm.

with the CNW load. Similar trends in T_g variations were observed in the case of cast films[21] and PS nanofibers loaded with gold nanoparticles.[17] However, the T_g measured for electrospun composite microfibers were relatively lower than those obtained for cast films filled with the same amount of CNW and surfactant. The difference in T_g between the CNW-loaded cast films and elecrospun nonwovens was also observed in the case of PS films and nanofibers filled with gold nanoparticles.[17] Finally, the reduction observed in T_g can be explained by the plasticizing effect of the surfactant.

A transition temperature was detected around 150°C for electrospun PS microfibers (see Fig. 6). This transition temperature increased with the addition of CNW stabilized by nonionic surfactant (around 160°C and 186°C for composites filled with 6% and 9% of CNW, respectively). One may argue that such observation can be the result of mechanical degradation of PS during sonication of CNW dispersions or other experimental artifacts. However, such explanations are to be ruled out because (1) we consistently observed this phenomenon in all repeated tests and, (2) the transition temperature was not identified in the case of cast films prepared with similar formulations. We hypothesize that the observed new transition is the result of the high voltage applied during the electrospinning process, which affected the structure of the polymer. In fact, such effect of the electrospinning process on the structure of the produced fibers has been reported for other polymers. For example, the crystallization of poly(L-lactide) (PLLA) was suppressed after electrospinning and no characteristic peak in both WAXD or in DSC was observed for the resulting

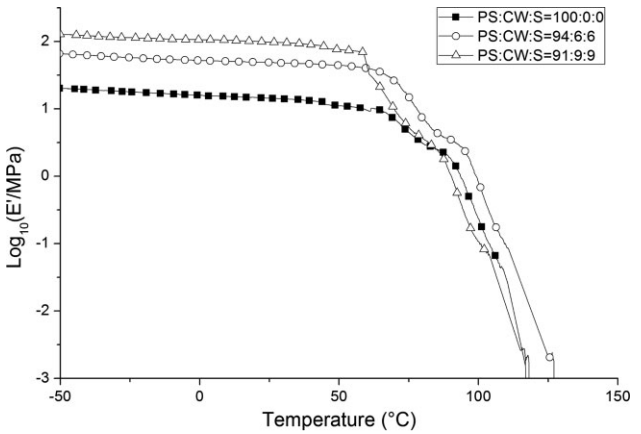

Figure 7 Storage modulus vs. temperature for electrospun microfibers collected as a nonwoven on a rotating mandril collector of neat PS and PS filler with 6 and 9% cellulose whiksers (CNW) in the presence of equivalent amount of nonionic surfactant (S). The electrospinning operating conditions were 20% PS in THF, $Q = 0.2$ mL/min, 40 kV, distance = 16 cm.

nanofibers.[37] A recent study by Yi et al. reported the same new transition (around 172°C) in polystyrene-grafted cellulose nanocrystals composites. The authors attributed this effect to liquid crystalline phase transitions. More detailed investigation is required to confirm these explanations in the case of CNW-loaded PS microfibers.[38]

Figure 7 shows the evolution with temperature of (the logarithm of) the storage tensile modulus, log (E'), in isochronal conditions at a frequency of 1 Hz for nonwovens produced by electrospinning and collected with the rotating mandril. All the curves were typical of an amorphous, high-molecular weight thermoplastic polymer. For temperatures below the glass transition region, the polymer matrix was in the glassy state and its storage modulus decreased slightly with temperature. The corresponding relaxation phenomenon at the glass transition temperature produced a drastic reduction in the storage tensile modulus; DMA measurement failed at above 125°C because of chain disentanglement effects.

Most distinctively, two transition temperatures were observed in the glass transition region during the DMA experiments (with all electrospun microfibers composites). The first temperature, ca. 90°C (for neat PS) or in the range of 87 to 85°C (for the PS filled with 6 and 9% CNW, respectively), corresponded to the glass transition temperature. These values corroborated the T_g values found in the case of the cast films.[21] The second transition temperature was observed at the onset of the storage modulus drop, at 64.7, 60.0, and 58.8°C for microfibers filled with 0, 6, and 9% of CNWs, respectively. This transition was not detected in the case of cast films.[21] It is hypothesized that this transition corresponds to the change in the microfiber state (undergoing untwisting), which is expected to occur under the combined effect of increased strain and temperature. A dramatic elongation occurred during this structural change and gave rise to a drastic drop in the storage modulus under increased stress.

DMA curves showed clearly the reinforcing effect of cellulose nanowhiskers in electrospun PS microfibers. The glassy modulus of electrospun PS microfibers filled with CNWs increased with CNW load. This reinforcing effect could be explained by the mechanical percolation phenomenon of cellulose nanowhiskers forming a stiff and continuous network held by hydrogen bonding.[39,40]

CONCLUSIONS

Nanoparticles (cellulose nanowhiskers) obtained from acid hydrolysis of cellulose were used to reinforce electrospun polystyrene micro and nanofibers. Nonionic surfactant sorbitan monostearate was successful to improve the dispersion properties of the hydrophilic reinforcing nanoparticle in the hydrophobic matrix and to produce bead-free electrospun composite webs. The obatined structures were characterized by scanning and transmission electron microscopy as well as dynamic mechanical analyses to reveal a number of features discussed here for the first time.

A significant effect of the cellulose nanowhiskers was the improved strength (elastic modulus) of the composite fibers. It was demonstrated that cellulose nanowhiskers can be used effectively as reinforcing material in electrospinning and to produce ribbon-shape fibers with unique structural properties. New temperature transitions were observed which were not present in the case of neat polystyrene matrices or composite cast (solid) films using same formulations. The manufactured nanocomposite fibers and respective nonwovens are of potential value given the highly porous structures they form and the large surface areas which are often required in high-performance applications.

References

1. Huang, Z. M.; Zhang, Y. Z.; Kotaki, M.; Ramakrishna, S. Compos Sci Technol 2003, 63, 2223.
2. Li, D.; Xia, Y. Adv Mater 2004, 16, 1151.
3. Teo, W. E.; Ramakrishna, S. Nanotechnology 2006, 17, R89.
4. Dersch, R.; Graeser, M.; Greiner, A.; Wendorff, J. H. Aust J Chem 2007, 60, 719.
5. Greiner, A.; Wendorff, J. H. Angew Chem 2007, 46, 5670.
6. Mares, L.; Petras, D.; Samek, L.; Cmelik, J. WO 2008/011,840 (2008).
7. Petras, D.; Maly, M.; Pozner, J.; Trdlicka, J.; Kovac, M. WO 2008/028,428-A1 (2008).
8. Petras, D.; Mares, L.; Stranska, D. WO 2006/131,081-A1 (2006).
9. Petras, D.; Mares, L.; Stranska, D.; Maly, M. WO 2007/054,039-A1 (2007).

10. Lee, K. H.; Kim, H. Y.; Bang, H. J.; Jung, Y. H.; Lee, S. G. Polymer 2003, 44, 4029.
11. Lin, T.; Wang, H.; Wang, H.; Wang, X. Nanotechnology 2004, 15, 1375.
12. Jarusuwannapoom, T.; Hongrojjanawiwat, W.; Jitjaicham, S.; Wannatong, L.; Nithitanakul, M.; Pattamaprom, C.; Koombhongse, P.; Rangkupan, R.; Supaphol, P. Eur Polym J 2005, 41, 409.
13. Pattamaprom, C.; Hongrojjanawiwat, W.; Koombhongse, P.; Supaphol, P.; Jarusuwannapoo, T.; Rangkupan, R. Macromol Mater Eng 2006, 291, 840.
14. Shin, D. S.; Lee, S. G.; Lyoo, W. S. Polym Compos 2006, 14, 755.
15. Wang, C.; Hsu, C.-H.; Lin, J.-H. Macromolecules 2006, 39, 7662.
16. Eda, G.; Liu, J.; Shivkumar, S. Eur Polym J 2007, 43, 1154.
17. Kim, J. K.; Ahn, H. Macromol Res 2008, 16, 163.
18. Pan, C.; Ge, L.-Q.; Gu, Z.-Z. Compos Sci Technol 2007, 67, 3271.
19. Sundaray, B.; Subramanian, V.; Natarajan, T. S. J Nanosci Nanotechnol 2007, 7, 1793.
20. Azizi Samir, M. A. S.; Alloin, F.; Dufresne, A. Biomacromolecules 2005, 6, 612.
21. Kim, J.; Montero, G.; Habibi, Y.; Hinestroza, J. P.; Genzer, J.; Argyropoulos, D. S.; Rojas, O. J. Compos Sci Technol, to appear.
22. Koombhongse, S.; Liu, W.; Reneker, D. H. J Polym Sci Part B: Polym Phys 2001, 39, 2598.
23. Liu, W.; Reneker, D. H. PMSE Prepr 2003, 88, 380.
24. Tao, J.; Shivkumar, S. Mater Lett 2007, 61, 2325.
25. Duan, H.-W.; Wang, Y.; Zhang, Y.-J.; Geng, L. J Polym Eng 2008, 28, 33.
26. Bazbouz, M. B.; Stylios, G. K. Eur Polym J 2007, 44, 1.
27. Gu, B. K.; Shin, M. K.; Sohn, K. W.; Kim, S. I.; Kim, S. J.; Kim, S.-K.; Lee, H.; Park, J. S. Appl Phys Lett 2007, 90, 263902/1.
28. Choi, S. S.; Chu, B.; Lee, S. G.; Lee, S. W.; Im, S. S.; Kim, S. H.; Park, J. K. J Sol–Gel Sci Technol 2004, 30, 215.
29. Fong, H.; Liu, W. D.; Wang, C. S.; Vaia, R. A. Polymer 2002, 43, 775.
30. Huang, C. B.; Chen, S. L.; Lai, C. L.; Reneker, D. H.; Qiu, H.; Ye, Y.; Hou, H. Q. Nanotechnology 2006, 17, 1558.
31. Wang, H.; Zhang, Y. P.; Shao, H. L.; Hu, X. C. J Mater Sci 2005, 40, 5359.
32. Zhang, C. X.; Yuan, X. Y.; Wu, L. L.; Han, Y.; Sheng, J. Eur Polym J 2005, 41, 423.
33. McCann, J. T.; Chen, J. I. L.; Li, D.; Ye, Z. G.; Xia, Y. A. Chem Phys Lett 2006, 424, 162.
34. Megelski, S.; Stephens, J. S.; Chase, D. B.; Rabolt, J. F. Macromolecules 2002, 35, 8456.
35. Liu, J. School of Polymer, Textile and Fiber Engineering; Georgia Institute of Technology: Atlanta, Georgia, 2007; p 245.
36. Dayal, P.; Liu, J.; Kumar, S.; Kyu, T. Macromolecules 2007, 40, 7689.
37. Kim, H. S.; Kim, K.; Jin, H. J.; Chin, I.-J. Macromol Symp 2005, 224, 145.
38. Yi, J.; Xu, Q.; Zhang, X.; Zhang, H. Polymer 2008, 49, 4406.
39. Dufresne, A. J Nanosci Nanotechnol 2006, 6, 322.
40. Dufresne, A. Can J Chem 2008, 86, 484.